

Resonantly enhanced photon-assisted tunneling in a multiple-quantum-well superlattice

G. S. Vieira* and S. J. Allen

Center for Terahertz Science & Technology, University of California, Santa Barbara, California 93106

P. S. S. Guimarães

Departamento de Física, Universidade Federal de Minas Gerais, Belo Horizonte, Brazil

K. L. Campman and A. C. Gossard

Materials Department, University of California, Santa Barbara, California 93106

(Received 26 June 1997)

Photon-assisted tunneling in a multiple-quantum-well superlattice is enhanced as the photon energy becomes resonant with the first intersubband transition. At resonance the process is characterized by tunneling from real states occupied by photoexcitation. Qualitative differences emerge between photon-assisted tunneling controlled by virtual states, under off-resonance conditions, and photon-assisted tunneling from real states, occupied by photoexcitation when on resonance.

[S0163-1829(98)10135-2]

INTRODUCTION

Photon-assisted transport in multiple-quantum-well (MQW) superlattices and laterally patterned nanostructures has emerged as a robust phenomenon with potential for THz detectors and THz sources.¹⁻⁶ In the presence of strong THz radiation, transport channels appear in a MQW superlattice corresponding to resonant tunneling into a neighboring well with the stimulated absorption or emission of one or more photons. Within the framework of sequential resonant tunneling, it appears that tunneling occurs through photon sidebands or virtual states. While the essential physics is captured in the work of Tien and Gordon's⁷ and Tucker's⁸ theory of photon-assisted transport in superconductor-insulator-superconductor (SIS) junctions, the basic transport mechanisms in semiconductor MQW superlattices are sufficiently different from their SIS analogs that new models of photon-assisted transport are being developed.⁹⁻¹³ The most important difference is the possibility of exciting sharp, well-defined, transitions within a quantum well. Analogous effects appear in the SIS junction when the photon energy exceeds the superconducting gap.¹⁴

As the photon energy is gradually brought into resonance with the intersubband transition in a quantum well, we expect the Tien-Gordon process of tunneling from virtual states to evolve into a process of tunneling between real states. One of these real states is only occupied by the absorption of a photon. The latter process has been extensively explored in the near infrared, at wavelengths of the order of 10 μm .¹⁵⁻²³ Here we experimentally explore the connection between these two processes, by monitoring the evolution of the photon-assisted process originating from a virtual state as we bring the photon energy into resonance with an intersubband transition. We show that the one-photon channels are *resonantly* enhanced when the photon energy coincides with the intersubband transition. Dynamic localization, the suppression of the 0.0-bias conductance and a dramatic feature of photon-assisted transport through photon sidebands, disappears and the conductance actually increases.

EXPERIMENTAL APPROACH

Photon-assisted transport appears most graphically as new features in the current-voltage (I - V) characteristics.¹⁻⁶ We key on three features in the current-voltage characteristics, sensitive to photon-assisted transport, and explore their dependence on resonance of the THz photon field with the first intersubband transition energy.

First we review the essential physics controlling the overall I - V characteristic. At low enough bias, the electron transport mechanism in a MQW superlattice occurs by resonant tunneling from the ground state of one well to the ground state of the next well ($1 \rightarrow 1$ in Fig. 1). At a bias where the current exceeds the maximum current for the $1 \rightarrow 1$ channel, two electric-field domains will be formed in the superlattice. In the low-field domain the electric transport will be $1 \rightarrow 1$, while in the high-field domain the electrons will tunnel from the ground state of one well to the first excited state of the next well ($1 \rightarrow 2$). In the bias region where the superlattice is divided into domains, the current does not change with the bias, i.e., there is a plateau in the I - V curve.²⁴ As the bias increases, so does the size of the high-field domain. Spikes in the plateau in the I - V curve can occur as the domain wall jumps from quantum well to quantum well. At some point the entire superlattice transports through the $1 \rightarrow 2$ channel and the current will increase again, until it saturates and a new high-field domain with resonant tunneling through $1 \rightarrow 3$ begins.

Applying intense THz radiation to a MQW superlattice causes sidebands to appear on quantum-well states, separated from a given real state by an integer multiple of the photon energy.⁷ This presents new channels to the current flow while diminishing others;^{1,3} new features appear in the I - V characteristic, while the conductance of other features is reduced.

On resonance with the intersubband transition, we expect the following new features to emerge. First, around zero bias, increasing the population of the second level should increase the contribution of the $2 \rightarrow 2$ channel, which is more conductive than the channel $1 \rightarrow 1$ [Fig. 1(a)]. (Off-

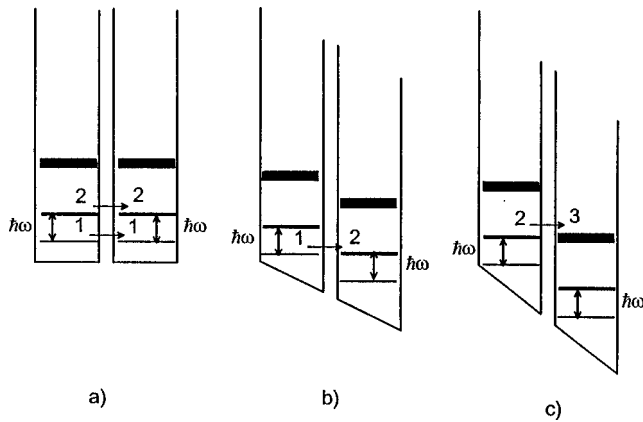


FIG. 1. Sequential resonant tunneling. (a) Near 0.0 V, tunneling occurs between equivalent states. On resonance the population of the excited state increases and the current increases. (b) Resonant tunneling between 1 and 2 is diminished when state 2 is populated by resonant excitation. (c) Photon-assisted tunneling from 1 to 3 is strongly enhanced when state 2 is photoexcited.

resonance, photon-assisted transport has the effect of diminishing the conductance near zero bias.³) Second, the channels $1 \rightarrow n$ should be inhibited by the depopulation of the ground state. But, when the electron transport is carried through the $1 \rightarrow 2$ channel, there is a further inhibition of the direct channel due to the increase in the population of second level [Fig. 1(b)]. Third, one-photon absorption from the first level of one well to the third level of the next well should be resonantly enhanced by photoexcitation to level 2 followed by direct tunneling, $2 \rightarrow 3$ [Fig. 1(c)]. Note that the first effect has the opposite sign to its off-resonant photon-assisted counterparts, while the first two are strongly resonant enhanced.

EXPERIMENT

We used a GaAs/Al_{0.3}Ga_{0.7}As superlattice, with ten wells and 11 barriers with a nominal thickness of 330/40 Å, respectively. On either side of the superlattice there are 500-Å GaAs spacers and 3000-Å GaAs contact layers. The superlattice and the spacers have a uniform nominal doping of $3 \times 10^{15} \text{ cm}^{-3}$ of Si, and the contact layers have a nominal doping of $2 \times 10^{18} \text{ cm}^{-3}$ of the same material. The sample was grown by molecular beam epitaxy on a semi-insulating GaAs substrate.

The resonant response was determined by varying the frequency of the THz radiation incident on the superlattice integrated into a bow-tie antenna. But the coupling of the radiation into the structure is a sensitive function of frequency, and normalizing the response by the incident power flux was unreliable. It proved far more effective to integrate a Schottky diode at the side of the superlattice device in a bow-tie antenna (Fig. 2). The antenna has one of the bows split in two, with one side connected to the superlattice and the other connected to the diode. Both the superlattice and the diode have an effective area of $2 \times 4 \mu\text{m}^2$. This design made it possible to bias the superlattice and Schottky devices independently while exciting with THz radiation. The source of THz radiation was the University of California at Santa

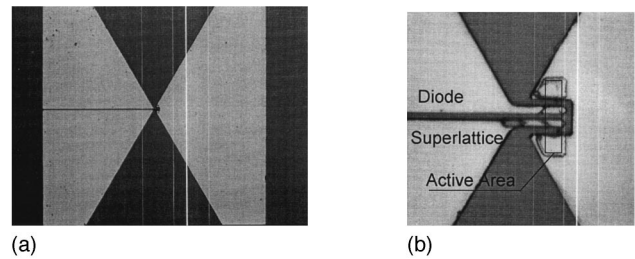


FIG. 2. (a) Light region is the metallization of the bow-tie antenna. The left bow is split, providing separate contact to the superlattice and Schottky detector. (b) The vertex of the antenna showing the active area and contacts to the superlattice and Schottky diode.

Barbara (UCSB) free-electron laser. All the experiments were performed with the sample at 20 K.

The spectroscopic measurement was made at a chosen power, fixed by the Schottky diode signal. Early experiments were made with the sample mounted over a hemispherical silicon lens. While this enhances the coupling of the radiation, it makes it hard to control the relative power falling on the two devices. Small changes in the angle of incidence cause large changes in relative signal. Removing the lens and irradiating from the antenna side of the substrate reduced the signal but produced reproducible results, relatively insensitive to the angle of incidence.

RESULTS AND DISCUSSION

We measured the frequency dependence of the three aforementioned features in the I - V characteristic: (1) the increase of conductivity around 0 V, (2) the decrease of current (negative photocurrent) in the $1 \rightarrow 2$ channel, and (3) a new plateau given by the appearance of the $2 \rightarrow 3$ channel.

In Figs. 3, 4, and 5 we show I - V curves, at the same radiation power (within 30%), but at radiation frequencies maximizing each of the three different features mentioned in the previous paragraph. Figure 3 shows the change of the slope of the I - V curve around zero bias, which occurs when the sample is illuminated with radiation resonant with the separation in energy between levels 1 and 2 of the quantum wells. At low bias, conduction through the superlattice occurs via $1 \rightarrow 1$ tunneling. The observed increase in the conductivity around zero bias results from resonant excitation of electrons from the first to second energy levels in the wells [Fig. 1(a)]. The increase in the population of the second level increases the overall conductivity, since the $2 \rightarrow 2$ tunneling is more effective than the $1 \rightarrow 1$ channel. This is apparent in the inset, where both the conductance at 0 V and the plateau, which represents the maximum current, supported by the channel increase substantially. *Virtual processes diminish the conductivity at 0 V. See Fig. 3 Ref. 3.*

Figure 4 shows that, at resonance, the current rise in the region of the I - V curve between the two first plateaus decreases. The inset shows the photocurrent (the difference between the I - V in the dark and the I - V under THz radiation) in that region. The width of the dip is controlled by the width of the quantum-well states involved in the resonant tunneling scaled by the number of quantum wells and leveraged by the contact regions. The drop in the current is attributed to inhibition of the $1 \rightarrow 2$ conduction channel caused by the reso-

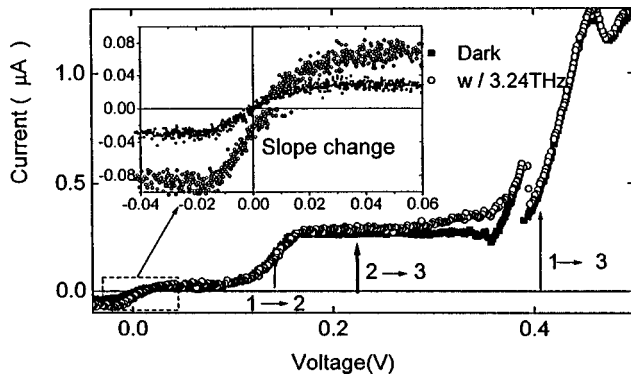


FIG. 3. Near 0.0 V, the current is enhanced on resonance reflecting the occupation of the first excited state that can support more current. The small offset is presumed to be due to rectification in the device or contacts. By design, there should be no offset, but inadvertent asymmetry in the superlattice or small departure from Ohmic behavior in the contact can cause this offset.

nant transfer of electrons from level 1 to level 2, as shown schematically in Fig. 1(b). As mentioned above, there is a double inhibition of the direct channel $1 \rightarrow 2$ due to both the depopulation of the ground state and the increase in the population of the second level. While photon-assisted transport through photon sidebands will also cause this effect, on resonance, the reduction in current for a given incident power is dramatically increased.

Lastly, in the region around 0.3 V, a new plateau appears that resembles the photon-induced plateau seen in photon-assisted tunneling off resonance, but it differs in an important respect. The plateau is seen at radiation powers much smaller than those needed for the onset of photon-assisted tunneling off resonance, and shows a strong frequency dependence, increasing dramatically as the frequency of the radiation is tuned to the transition between the first two energy levels. We interpret the new plateau as being due to a new conduction channel, tunneling from level 2 to level 3 ($2 \rightarrow 3$), made possible by photoexcitation to the second level, as depicted in Fig. 1(c). It does occur at the position expected for the direct photon-assisted transport from 1 to 3 but the resonant photon-assisted tunneling is much more efficient than the direct photon-assisted tunneling. Since the

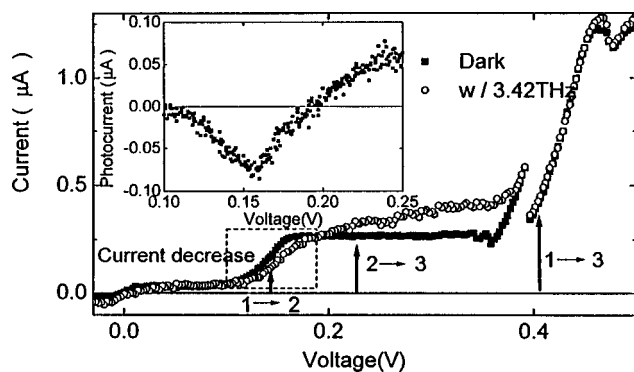


FIG. 4. The current at the $1-2$ step is diminished by depletion of the ground state and occupation of the first excited state.

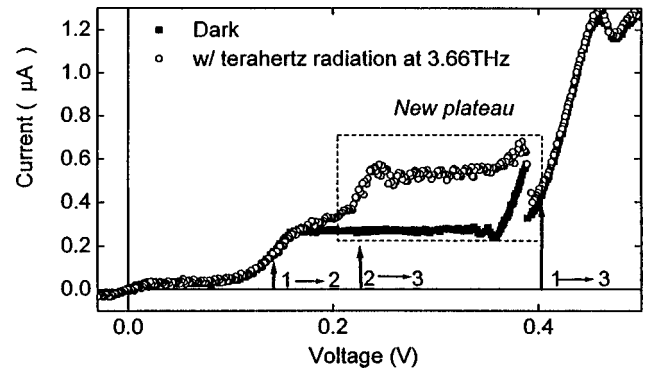


FIG. 5. A new plateau occurs at the same position as the $1-3$ photon-assisted plateau. But it requires substantially less power, since the feature is promoted by the photoexcitation of state 2 followed by direct tunneling to state 3.

two processes are quite different, it should come as no surprise that the power required to see the off-resonant channels is different from the resonant intersubband absorption. The latter can saturate on resonance at powers well below that required to turn on the transport through virtual photon sidebands.

It is also interesting to note that the current corresponding to the $1 \rightarrow 3$ channel (the region between the second and third plateaus, with a dc bias between 0.40 and 0.45 V) does not change significantly with the radiation at the power level used in Figs. 3, 4, and 5. This implies that the power used is much smaller than that necessary to disturb the direct conduction channels off resonance.

The three effects on the $I-V$ characteristics, shown in Figs. 3, 4, and 5, are strongly frequency dependent. Their frequency dependence is shown in Fig. 6.

The resonance frequency is not the same for the three effects. This is due to the fact that the features observed occur at different biases. Since the shape of the quantum wells is electric field dependent, we expect the resonance to depend on electric field. The nominal values of the superlattice (40-Å barriers and 330-Å wells) give us a resonant frequency between the two first levels of 3.05 THz at zero applied dc electric field. The measured resonance at zero bias is 3.27 THz. If we adjust the well width from 330 to 317 Å, the calculated resonance at zero bias matches the measured value. Using this value of well width, we calculated the frequency at which we should expect each of the features to occur, taking into account the change in the level separation with the electric field and assuming a uniform electric field. Arrows in Figs. 3, 4, and 5 indicate the corresponding biases.

In Fig. 7 we show, along with the measured resonances, the calculated electric-field dependence of the resonance for a superlattice with the nominal and with the modified well width. The experimentally observed dependence on electric field is reproduced by the model calculation with a modified well width.

The process of resonantly enhanced photon-assisted tunneling is basically an intersubband transition, and should saturate at some power. In Fig. 8, we show the power dependence of the three resonance peaks of Fig. 6. Saturation is clearly seen. The arrows show the power at which the spectroscopic measurement reported here was made. Once more

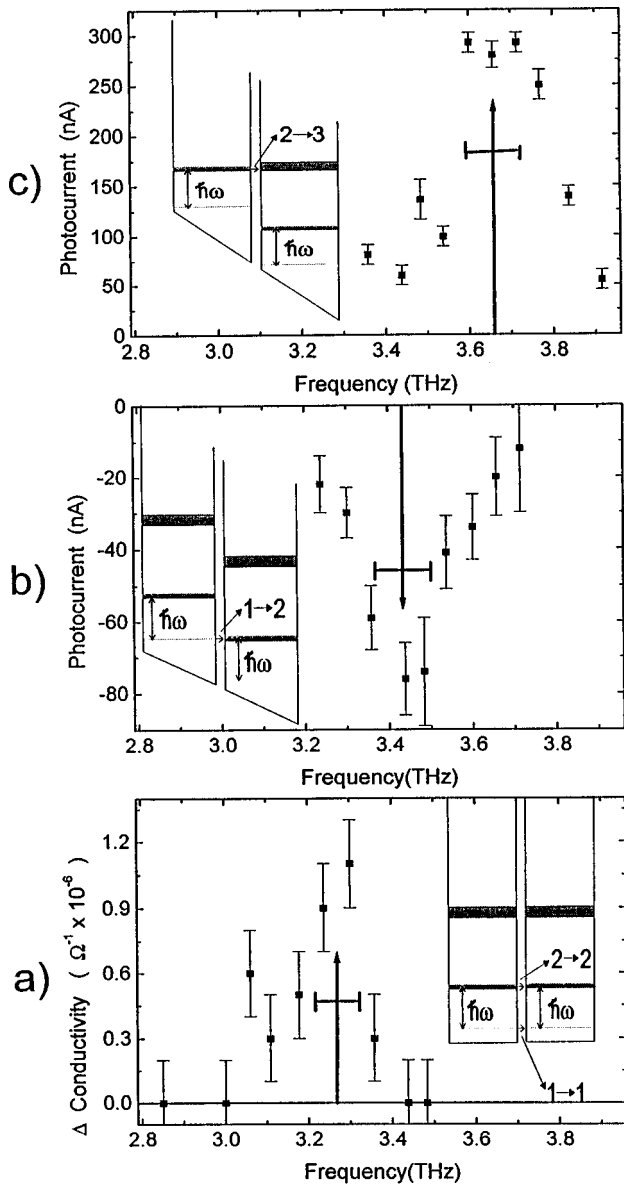


FIG. 6. The features shown in Figs. 3, 4, and 5 are resonant at slightly different frequencies, since they are observed at different bias conditions.

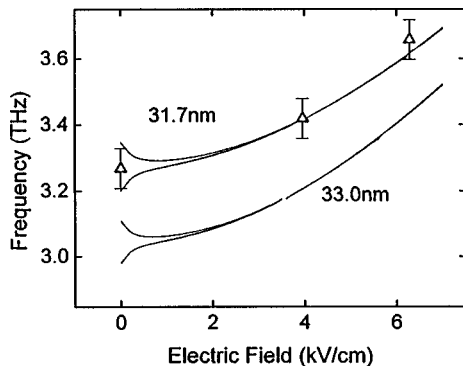


FIG. 7. Resonant frequency vs superlattice electric field. To achieve quantitative agreement, the quantum wells are assumed to be 31.7 nm rather than the nominal 33.0 nm.

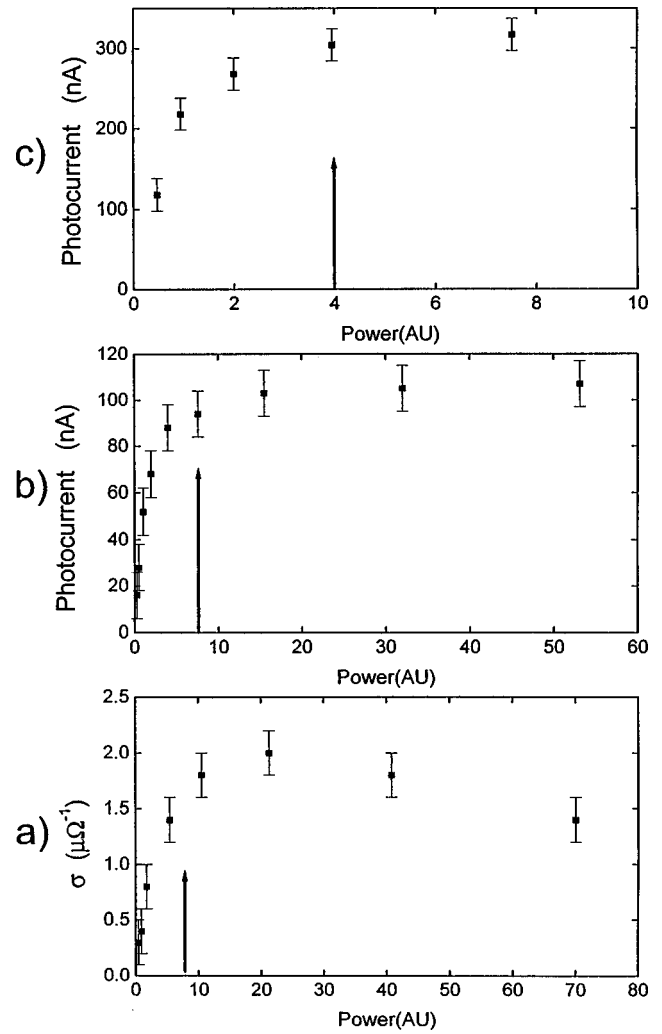


FIG. 8. The resonant features appear to saturate as a function of THz power. (a), (b), and (c) correspond to the figures shown in Fig. 6. Note that the horizontal scales differ in the three plots.

we see that the features do not behave as photon-assisted tunneling off resonance, since the power dependence does not follow a Bessel-function-like behavior.³

CONCLUSION

We have observed the evolution of THz photon-assisted transport in multiple-quantum-well superlattices as the radiation field comes on resonance with the first intersubband transition. On resonance, the radiation effects the *I-V* characteristics in a qualitatively different manner than when off resonance. These results distinguish experimentally photon-assisted transport via photon sidebands and virtual states, from photon-assisted transport via tunneling from real states occupied by photoexcitation. The resonance is shifted by the applied dc bias, in agreement with a model based on the dc Stark effect. In the future it will be important to explore interference between tunneling from real states occupied by photoexcitation and tunneling from virtual states, but it is apparent that this will require barriers sufficiently thin that the photon-assisted process is as important as the resonant intersubband channel.

ACKNOWLEDGMENTS

We would like to thank Jeff S. Scott for his help with the software used to perform the experiments, Thomas Fromherz for his help with the calculations of the level positions, and the whole staff of UCSB Free Electron Laser Studies, J. R.

Allen, D. Enyeart, G. Ramian, and D. White, for their outstanding support, commitment, and expertise. G.S.V. and P.S.S.G. also would like to thank Conselho Nacional de Desenvolvimento Científico e Tecnológico (CNPq), Brazil, for financial support. Research at UCSB was supported by ONR and AFOSR.

*On leave from Universidade Federal de Minas Gerais, Brazil.

- ¹P. S. S. Guimarães, B. J. Keay, J. P. Kaminski, S. J. Allen, Jr., P. F. Hopkins, A. C. Gossard, L. T. Florez, and J. P. Harbison, *Phys. Rev. Lett.* **70**, 3792 (1993).
- ²B. J. Keay, P. S. S. Guimarães, J. P. Kaminski, S. J. Allen, Jr., P. F. Hopkins, A. C. Gossard, L. T. Florez, and J. P. Harbison, *Surf. Sci.* **305**, 385 (1994).
- ³B. J. Keay, S. J. Allen, Jr., K. D. Maranowski, A. C. Gossard, U. Bhattacharya, and M. J. M. Rodwell, *Phys. Rev. Lett.* **75**, 4102 (1995).
- ⁴S. Zeuner, B. J. Keay, S. J. Allen, K. D. Maranowski, A. C. Gossard, U. Bhattacharya, and M. J. W. Rodwell, *Phys. Rev. B* **53**, 1717 (1996).
- ⁵K. Unterrainer, B. J. Keay, M. C. Wanke, S. J. Allen, D. Leonard, G. Medeiros-Ribeiro, U. Bhattacharya, and M. J. W. Rodwell, *Phys. Rev. Lett.* **76**, 2973 (1996).
- ⁶H. Drexler, J. S. Scott, S. J. Allen, K. L. Campman, and A. C. Gossard, *Appl. Phys. Lett.* **67**, 2816 (1995).
- ⁷P. K. Tien and J. P. Gordon, *Phys. Rev.* **129**, 647 (1963).
- ⁸J. R. Tucker, *IEEE J. Quantum Electron.* **QE-15**, 1234 (1979).
- ⁹C. A. Stafford and Ned S. Wingreen, *Phys. Rev. Lett.* **76**, 1916 (1996).
- ¹⁰A. Wacker, F. Prengel, and E. Chöll, in *Physics of Semiconductors: Proceedings of the 22nd International Conference*, edited by D. J. Lockwood (World Scientific, Singapore, 1995), Vol. 2, p. 1075.
- ¹¹M. Wagner, *Phys. Rev. Lett.* **76**, 4010 (1996).
- ¹²B. J. Keay and C. Aversa, *Phys. Rev. B* **54**, R2284 (1996).
- ¹³Y. Dakhnovskii and H. Metiu, *Phys. Rev. B* **51**, 4193 (1995).
- ¹⁴G. de Lange, C. E. Honingh, J. J. Kuipers, H. H. A. Schaeffer, R. A. Panhuizen, T. M. Klapwijk, H. van de Stadt, and M. M. W. M. de Graauw, *Appl. Phys. Lett.* **64**, 3039 (1994).
- ¹⁵B. F. Levine, K. K. Choi, C. G. Bethea, J. Walker, and R. J. Malik, *Appl. Phys. Lett.* **50**, 1092 (1987).
- ¹⁶K.-K. Choi, B. F. Levine, C. G. Bethea, J. Walker, and R. J. Malik, *Appl. Phys. Lett.* **50**, 1814 (1987).
- ¹⁷B. F. Levine, K. K. Choi, C. G. Bethea, J. Walker, and R. J. Malik, *Appl. Phys. Lett.* **51**, 934 (1987).
- ¹⁸B. F. Levine, C. G. Bethea, K. K. Choi, J. Walker, and R. J. Malik, *Appl. Phys. Lett.* **53**, 231 (1988).
- ¹⁹B. F. Levine, C. G. Bethea, G. Hasnain, J. Walker, and R. J. Malik, *Appl. Phys. Lett.* **53**, 296 (1988).
- ²⁰A. Larsson, S. I. Borenstain, B. Jonsson, I. Andersson, J. Westin, and T. G. Andersson, *Appl. Phys. Lett.* **58**, 1297 (1991).
- ²¹H. Schneider, F. Fuchs, B. Dischler, J. D. Ralston, and P. Koidl, *Appl. Phys. Lett.* **58**, 2234 (1991).
- ²²J. Y. Duboz, E. Costard, J. Nagle, J. M. Berset, J. M. Ortega, and J. M. Gérard, *J. Appl. Phys.* **78**, 1224 (1995).
- ²³C. Mermelstein and A. Sa'ar, *Superlatt. Microstruct.* **19**, 375 (1996).
- ²⁴K. K. Choi, B. F. Levine, R. J. Malik, J. Walker, and C. G. Bethea, *Phys. Rev. B* **35**, 4172 (1987).